

# Catalytic behaviour of $\text{La}_4\text{PdO}_7$ based catalysts when exposed to car exhaust conditions

M. Andersson, K. Jansson and M. Nygren<sup>1</sup>

*Inorganic Chemistry, Arrhenius Laboratory, Stockholm University, S-10691 Stockholm, Sweden*

Received 29 September 1995; accepted 29 February 1996

The catalytic properties of ex situ prepared  $\text{La}_4\text{PdO}_7$  were studied under automotive exhaust conditions. Monophasic  $\text{La}_4\text{PdO}_7$  was deposited onto  $\gamma\text{-Al}_2\text{O}_3$  coated cordierite monoliths and light-off curves were recorded under oxidising and reducing conditions. Initially the catalytic activity for oxidation of CO and  $\text{C}_3\text{H}_6$  and reduction of NO was low but after the catalyst had been exposed to a reducing atmosphere of simulated car exhaust composition at 600°C a three-way catalytic behaviour was obtained with a  $T_{50}$  value of about 340°C. Using oxidising conditions and a similar activation procedure, a catalyst with CO and  $\text{C}_3\text{H}_6$  oxidation activity ( $T_{50} = 405^\circ\text{C}$ ) but minor activity for reduction of NO was obtained. This behaviour is interpreted in terms of  $\text{La}_4\text{PdO}_7$  being decomposed and nanosized PdO particles being formed; these in turn are reduced to Pd and Pd is the catalytically active component in the catalyst. These conclusions are supported by X-ray diffraction, infrared spectroscopy, scanning and transmission electron microscopy studies combined with element analysis of freshly prepared and thermally activated catalysts.

**Keywords:** catalysis;  $\text{La}_4\text{PdO}_7$ ; Pd; PdO; TWC behaviour

## 1. Introduction

A commercial car exhaust catalyst typically contains Pt and Rh in a ratio of 5 : 1, which is substantially different from the natural occurrence of these metals (approximately 19 : 1). Even though the amount of noble metals used in a commercial car exhaust catalyst is small (~2.5 mg per gram catalyst) the price of Rh is high. Thus, there is a demand to find another material which, as Rh, selectively reduces  $\text{NO}_x$ . Palladium is an excellent catalyst for oxidation of CO and hydrocarbons and it has been found that Pd, freshly deposited on an  $\text{Al}_2\text{O}_3$  substrate, does reduce  $\text{NO}_x$  to  $\text{N}_2$  and  $\text{O}_2$  but that such a catalyst easily becomes aged, i.e. exhibits a comparatively low activity for reduction of  $\text{NO}_x$  due to hydrocarbon poisoning [1]. However, the addition of  $\text{La}_2\text{O}_3$  to this catalyst improves the  $\text{NO}_x$  reducing activity substantially [1–6], i.e. the hydrocarbon poisoning effect is suppressed.

The mechanism of interaction between Pd and  $\text{La}_2\text{O}_3$  is not yet fully understood. However, temperature-programmed reduction (TPR) and decomposition (TPD) experiments have suggested that the addition of  $\text{La}_2\text{O}_3$  to a palladium catalyst stabilised the oxidised form of palladium [1,2]. Hoost et al. have pointed out that some La–Pd oxide could be present at the interface between  $\text{La}_2\text{O}_3$  and Pd, which in turn would stabilise the oxidised form of palladium [2].

According to Kakhan et al. there are three stoichiometric compounds in the pseudo-binary system  $\text{La}_2\text{O}_3$ –PdO, namely  $\text{La}_4\text{PdO}_7$ ,  $\text{La}_2\text{Pd}_2\text{O}_5$  and  $\text{La}_2\text{PdO}_4$  [7]. All

three compounds have higher thermal stability than pure PdO, which decomposes around 800°C in air, and of these  $\text{La}_4\text{PdO}_7$  has the highest decomposition temperature (1310°C).

In this article we report on the catalytic activity of a material of the overall composition  $\text{La}_4\text{PdO}_7$  for oxidation of CO and  $\text{C}_3\text{H}_6$  and reduction of NO. Monophasic  $\text{La}_4\text{PdO}_7$  has been synthesised ex situ and deposited onto a  $\gamma\text{-Al}_2\text{O}_3$  washcoat. The morphology and composition of the catalysts, before and after being activated in the reactor test chamber, have been studied in a scanning electron microscope (SEM) and in an analytical transmission electron microscope (ATEM), both provided with energy dispersive spectrometers (EDS). The phases have been identified by their X-ray powder diffraction patterns and by infrared spectroscopy studies.

## 2. Experimental

### 2.1. Materials

The following starting materials were used:  $\text{La}(\text{NO}_3)_3 \cdot 6\text{H}_2\text{O}$  (p.a., Merck), anhydrous  $\text{PdCl}_2$  (purum, Fluka), HCl (fuming 37% p.a., Merck), Dispersal alumina powder of boehmite (Condea chemie), cordierite monoliths having a honeycomb structure with 64 quadratic channels per  $\text{cm}^2$  (Corning Glass) and *n*-butyl alcohol (p.a., May & Baker LTD). *n*-hexane (p.a., Merck), was used for sample storage (see below) and KBr (p.a., Merck) for IR-spectroscopy sample preparation. The gases NO, He, CO,  $\text{O}_2$  and propene used in the test reactor were supplied by AGA Gas AB.

<sup>1</sup> To whom correspondence should be addressed.

## 2.2. Catalyst preparation

Monophasic  $\text{La}_4\text{PdO}_7$  samples were prepared as follows; (i) lanthanum nitrate and palladium chloride were dissolved in fuming hydrochloric acid in a molar ratio of 4 : 1 and the solution was boiled to dryness; (ii) the residue was slowly heated to 550°C and held at this temperature for 2 h; (iii) the temperature was then raised to 1000°C and the samples were heat treated at this temperature for 1–3 days.

A boehmite slurry of Dispersal alumina powder was prepared by dispersing 15 g of the powder in a mixture of 100 cm<sup>3</sup> deionised water and 1 cm<sup>3</sup> concentrated hydrochloric acid. Monolith samples with a length of 15 mm and a cross section containing 69 square channels were cut from the commercial honeycomb structure of cordierite. The channels were furnished with a porous support of alumina by a dip-coating procedure as described elsewhere [8]. The washcoat was calcined at 550°C in air for 1 h and the alumina content was then 1.4–2.0 wt%. The prepared  $\text{La}_4\text{PdO}_7$  was ground in a mortar and mixed with *n*-butyl alcohol. The mixture was subjected to ultrasonic treatment for a couple of minutes to avoid formation of agglomerates. The monoliths provided with alumina supports were dipped in the  $\text{La}_4\text{PdO}_7$  slurry and then allowed to dry in an oven at 150°C with the channels in a horizontal position. This procedure was repeated until the loading of palladium was in the range 0.96–1.1 wt%. The catalysts were finally heat treated at 900°C for 24 h.

## 2.3. Characterisation

The ex situ prepared  $\text{La}_4\text{PdO}_7$  samples were characterised by their X-ray powder patterns obtained in a Guinier-Hägg camera, using  $\text{Cu K}\alpha_1$  radiation and Si as internal standard. The obtained photographs were evaluated in a computerised scanner system [9] and the obtained records were matched with tabulated JCPDS data. Samples for characterization of the catalysts which had been subjected to reactor tests were obtained by gently scratching off material from the surface of the channels of the monolith. The scratched-off material was studied immediately or stored under hexane in order to minimise the possibility of a reaction between atmospheric moisture and formed  $\text{La}_2\text{O}_3$ . The crystalline phases present in these samples were identified by their X-ray diffraction patterns. FT-IR spectra of some of these materials were recorded in the range 4000–370 cm<sup>-1</sup> on a Bruker IFS 55 spectrometer equipped with a KBr beamsplitter and DGS and PbS detectors for mid-IR and near-IR, respectively, using the KBr tablet sample preparation technique.

The morphology of the  $\text{La}_4\text{PdO}_7$  and its particle distribution on the support were studied in two SEMs (Jeol 820 and 880) both equipped with EDS detectors (LINK AN 10000). ATEM (Jeol 2000FX furnished

with the same type of EDS detector) studies were carried out to characterise the ex situ prepared  $\text{La}_4\text{PdO}_7$  crystals and the catalysts which had been subjected to reactor tests.

## 2.4. Reactor and testing procedure

The catalytic tests were performed in a gas flow reactor using the gas compositions given in table 1, which were introduced into the reactor via mass flow controllers (Bronkhorst HI-TEC type F-201C-FA-22-V and -P). The light-off performance was studied by increasing the reactor gas temperature from 100 to 650°C at a constant rate of 6°C/min, monitoring the temperature by two thermocouples, one placed in front of and one behind the catalyst. Reactant and product gases were analysed and recorded on-line with a mass spectrometer (Balzers QMG 420) connected to a PC. The detector response on selected mass numbers was recorded as function of the inlet gas temperature, and for intercomparison of the recorded curves the following normalisation procedure was performed. Firstly the background level was measured at the mass number 50 and subtracted from all signals. To account for pressure changes in the mass chamber during the reactor runs, the signals were normalised using the helium signal as an internal standard. Assuming that no catalytic activity occurred at the starting point ( $T = 100\text{--}120^\circ\text{C}$ ) the signals were finally divided by their starting value. The obtained data were then converted to degree of conversion. For the sake of comparison, the light off curves for CO,  $\text{C}_3\text{H}_6$  and NO of a commercial TWC containing 2.1 mg Pt/Rh per g catalyst (with a Pt : Rh ratio of 5 : 1) are plotted in each graph. The light-off temperature,  $T_{50}$ , for each reactant is defined as the temperature of the inlet gas where 50% of the observed maximum conversion of each reactant occurs.

The stoichiometric number,  $S$ , used as a redox characteristic of the feed stream, is defined as in ref. [10] with all concentrations expressed in vol%:

$$S = (2[\text{O}_2] + [\text{NO}]) / ([\text{CO}] + 9[\text{C}_3\text{H}_6])$$

For  $S < 1$  and  $S > 1$  the gas mixture is reducing and oxidising, respectively.  $S$  values of 0.9 and 1.1 have been used.

Table 1  
Composition of the gas feed streams used

$S$	Composition of gas mixture (vol%) <sup>a</sup>			
	$\text{O}_2$	NO	CO	$\text{C}_3\text{H}_6$
0.9	0.771	0.097	1.56	0.029
1.1	0.954	0.097	1.56	0.029

<sup>a</sup> All given compositions are balanced with He to yield a space velocity of 59 000 h<sup>-1</sup>.

### 3. Results and discussion

#### 3.1. Catalytic behaviour

The catalytic behaviour of freshly prepared  $\text{La}_4\text{PdO}_7$  in reducing atmosphere ( $S = 0.9$ ) is shown in fig. 1. From the figure it can be seen that this catalyst has very small or no activity for oxidation of CO and  $\text{C}_3\text{H}_6$  as well as for reduction of NO (first run). However, if the same catalyst was exposed to reducing atmosphere ( $S = 0.9$ ) for half an hour at  $600^\circ\text{C}$ , cooled to  $100^\circ\text{C}$  in the same atmosphere and re-heated as above and this procedure was repeated several times, the catalytic activity increased cycle by cycle so as to yield reproducible light-off curves after the fourth cycle, as seen in fig. 1. A typical three-way catalytic (TWC) behaviour was observed in the latter case, with  $T_{50} = 340^\circ\text{C}$ .

Corresponding light-off curves for the same type of catalyst in oxidising atmosphere ( $S = 1.1$ ) are shown in fig. 2. Again, freshly prepared  $\text{La}_4\text{PdO}_7$  did not exhibit any appreciable catalytic activity, but very nearly reproducible oxidative behaviour was observed when the catalyst had been cycled seven times, yielding a  $T_{50}$  about  $405^\circ\text{C}$  for oxidation of CO and  $\text{C}_3\text{H}_6$  but only a very moderate activity for reduction of NO. If this activated catalyst is re-heated at  $900^\circ\text{C}$  in air for 1 h one obtains light-off curves similar to those found after the second and third cycle in the activation procedure of freshly prepared  $\text{La}_4\text{PdO}_7$ . Thus re-heat treatment of an activated catalyst yielded a catalyst with lower activity for oxidation of CO and  $\text{C}_3\text{H}_6$  and higher  $T_{50}$  values. When the latter catalyst was cycled, the oxidation activity increased and an almost reproducible behaviour was reached after the fifth cycle with  $T_{50}$  values for oxidation of CO and  $\text{C}_3\text{H}_6$  in the same range as above. Again, very small or no activity for reduction of NO was observed.

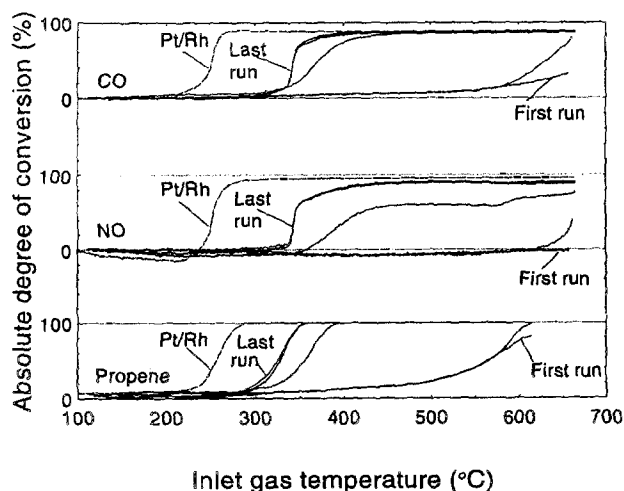


Fig. 1. Degree of conversion of CO,  $\text{C}_3\text{H}_6$  and NO as function of the inlet temperature of the gas over  $\text{La}_4\text{PdO}_7$  obtained in reducing atmosphere ( $S = 0.9$ ). Reproducible conversion curves were obtained after the fourth cycle (see text).

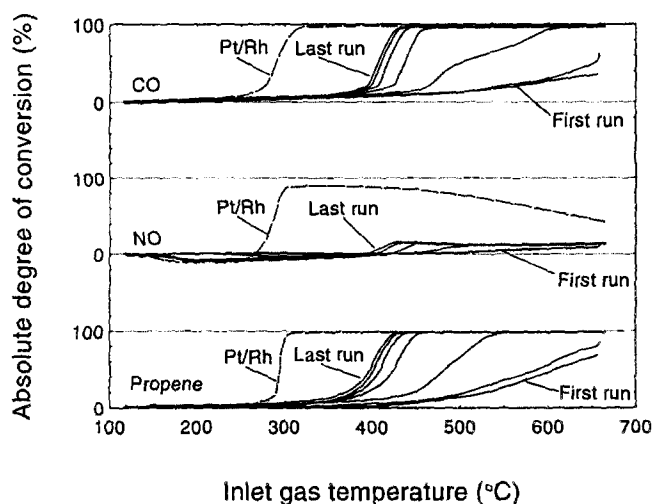


Fig. 2. Degree of conversion of CO,  $\text{C}_3\text{H}_6$  and NO as function of the inlet temperature of the gas over  $\text{La}_4\text{PdO}_7$ , obtained in oxidising atmosphere ( $S = 1.1$ ). Reproducible conversion curves were obtained after the fifth cycle (see text).

Another activation route was also tested. A freshly prepared catalyst was exposed to reducing atmosphere ( $S = 0.9$ ) at  $600^\circ\text{C}$  for 1 h, and cooled slowly to a temperature below the  $T_{50}$  value for the TWC behaviour observed above ( $340^\circ\text{C}$ ), held at this temperature ( $\sim 300^\circ\text{C}$ ) for at least 1 h. Typically this procedure lasted for 5 h. After this procedure the same cycling procedure as described above was applied, and when the catalyst had been cycled once the light-off curves were very similar to the ones obtained after four cycles above. These findings imply that the procedure to obtain an activated catalyst is so far not optimised and experiments aimed at exploring the reactions involved in the activation procedure are being undertaken.

#### 3.2. Phase analysis

The X-ray powder pattern of the ex situ prepared sample of  $\text{La}_4\text{PdO}_7$  could be ascribed to  $\text{La}_4\text{PdO}_7$  with unit cell parameters ( $a = 13.475$ ,  $b = 4.031$ ,  $c = 9.451$  Å and  $\beta = 133.41$ ) in close agreement with those reported by Attfield and Férey [11]. The powder pattern also contained a few very weak reflections (with intensities  $< 2\%$  of the strongest  $\text{La}_4\text{PdO}_7$  peak) that could be ascribed to  $\text{La}(\text{OH})_3/\text{La}_2\text{O}_3$ . The colour of the sample was light brown as reported for  $\text{La}_4\text{PdO}_7$  by Kakhan et al. [7].

The channels of the catalysts activated under reducing conditions revealed a 3 mm long light brown field at the gas inlet side, while the remaining parts had a black colour. The light brown colour matched exactly the colour of the freshly prepared  $\text{La}_4\text{PdO}_7$ , and the X-ray powder patterns of materials gently scratched off from the differently coloured sections could be ascribed to  $\text{La}_4\text{PdO}_7$  (the light brown part) and  $\text{La}_2\text{O}_3$  (the black part). Material that had been activated under reducing conditions and re-heated at  $900^\circ\text{C}$  in air for one hour

exhibited an X-ray powder pattern that was identical with that of  $\text{La}_4\text{PdO}_7$ .

### 3.3. SEM and ATEM studies

The SEM studies showed that the formed  $\text{La}_4\text{PdO}_7$  particles were in the micron to sub-micron size range and that they were evenly distributed on the  $\text{Al}_2\text{O}_3$  washcoat. Backscattered electron images of these samples viewed in profile showed that the  $\text{La}_4\text{PdO}_7$  layer was 5–10  $\mu\text{m}$  thick.

The ATEM studies of the freshly prepared  $\text{La}_4\text{PdO}_7$  revealed the presence of smoothly shaped crystals with an La: Pd ratio of 4:1 and exhibiting lattice fringe images (see fig. 3) while the morphology of activated particles was quite different (see fig. 4). Comparing figs. 3 and 4 one observes that the outer part of the crystals exposed to oxidizing atmosphere is more distorted than that of the as-prepared ones. The ATEM studies of the former material revealed the presence of a few ( $\sim 5\%$ )  $\text{La}_4\text{PdO}_7$  particles which had approximately 20 nm large crystals on their surfaces, as illustrated in fig. 5. EDS analysis of these nano-crystallites yielded pure EDS-Pd signals suggesting them to be Pd or PdO particles.

Material activated in reducing atmosphere and then transferred directly to the microscope exhibited smooth particles with a fluffy surface structure containing small Pd/PdO particles in sizes up to 20 nm, as seen in fig. 6.

### 3.4. FT-IR studies

In an attempt to establish whether the nano-sized particles seen in the ATEM studies were Pd or PdO, IR

spectra of PdO,  $\text{La}(\text{OH})_3$ ,  $\text{La}_2\text{O}_3$ , and  $\text{La}_4\text{PdO}_7$  as prepared and activated under oxidizing and reducing conditions were recorded. The obtained spectra are given in fig. 7. It was found that: (i) PdO absorbs in the region 680–570  $\text{cm}^{-1}$ ; (ii)  $\text{La}(\text{OH})_3$  has absorption peaks at 3600 and 700–600  $\text{cm}^{-1}$ ; (iii)  $\text{La}_4\text{PdO}_7$  absorbs in the range 500–600  $\text{cm}^{-1}$ ; (iv)  $\text{La}_2\text{O}_3$  has no interfering peaks at these wavenumbers. The amount of PdO used to obtain the spectrum given in fig. 7a was in the same range as that expected to be present in the tablets of activated materials if they were fully decomposed to  $\text{La}_2\text{O}_3$  and PdO.

The spectrum of the material activated under reducing conditions and rapidly incorporated in the KBr tablet (fig. 7e) can be interpreted in terms of  $\text{La}_4\text{PdO}_7$  being decomposed to  $\text{La}_2\text{O}_3$  and Pd under reducing conditions while the spectrum given in fig. 7f suggests that  $\text{La}_4\text{PdO}_7$  and possibly minor amounts of PdO and  $\text{La}_2\text{O}_3$  are present in samples activated under oxidizing conditions. The spectrum of the sample activated under reducing conditions and stored in a desiccator provided with silica gel showed the presence of  $\text{La}(\text{OH})_3$ .

These observations suggest that the darker grains seen in the ATEM studies are Pd particles rather than PdO.

## 4. Concluding remarks

The  $\text{La}_4\text{PdO}_7$  lattice consists of a distorted, primitive cubic network of oxygen ions containing face- and body-centred  $\text{Pd}^{2+}$  and  $\text{La}^{3+}$  ion networks, respectively [12]. Atterfield and Férey have shown that the PdO,

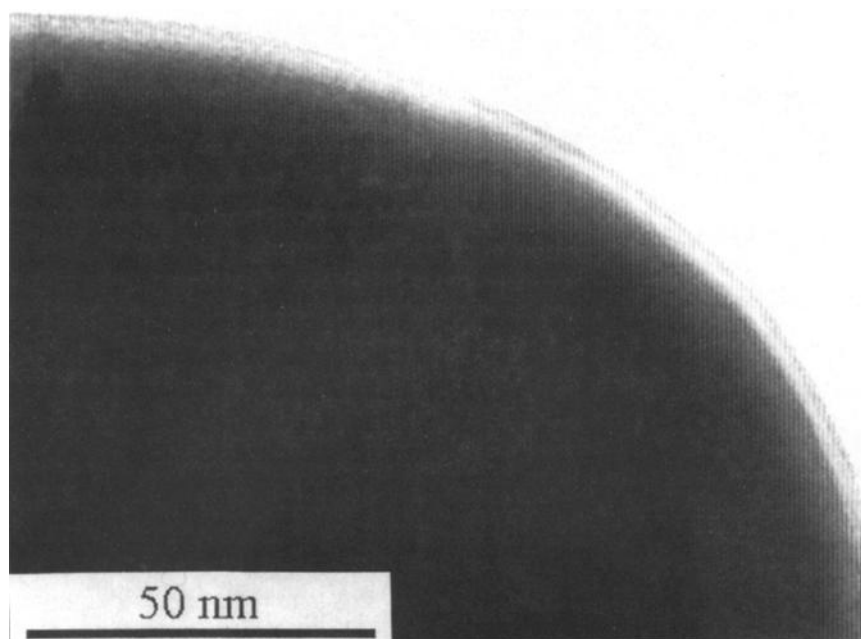


Fig. 3. A TEM image of a freshly prepared  $\text{La}_4\text{PdO}_7$  crystal.

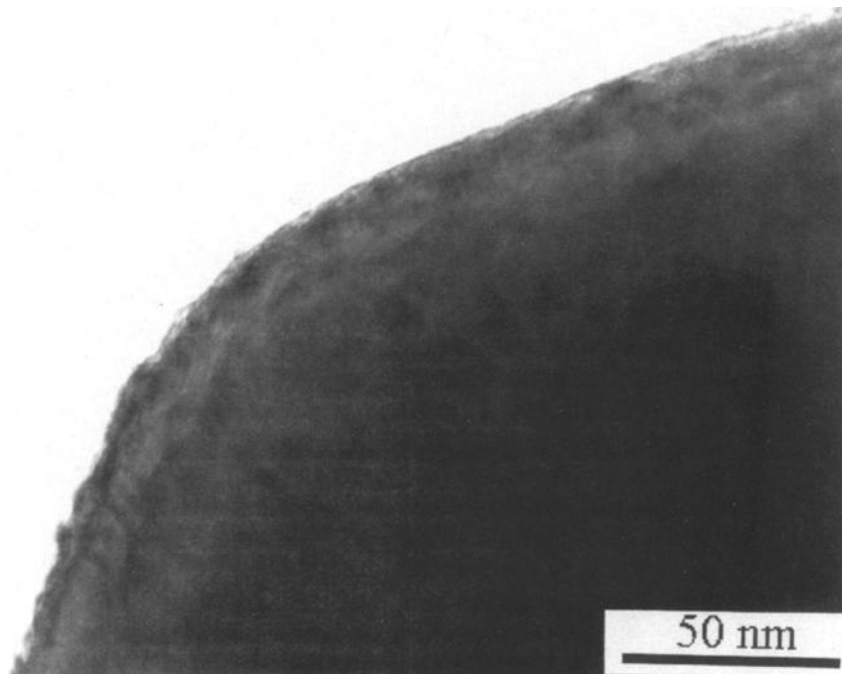


Fig. 4. A TEM image of an  $\text{La}_4\text{PdO}_7$  particle which has been exposed to oxidising atmosphere ( $S = 1.1$ ).

$\text{La}_2\text{Pd}_2\text{O}_5$ ,  $\text{La}_2\text{PdO}_4$ ,  $\text{La}_4\text{PdO}_7$  and  $\text{La}_2\text{O}_3$  structures are members of a series of the composition  $\text{La}_{2n}\text{Pd}_2\text{O}_{3n+2}$  with  $n = 0, 1, 2, 4$  and  $\infty$ , respectively [11]. The ternary compounds can be regarded as ordered intergrowths of  $\text{PdO}$  and  $\text{La}_2\text{O}_3$ . In  $\text{La}_4\text{PdO}_7$ , isolated  $\text{PdO}_4$  square planes run along the  $[201]$  direction of the unit cell. Atterfield and Férey have also shown that the different structures can be generated by removals or

additions of  $\text{PdO}$  and/or  $\text{La}_2\text{O}_3$  units along defined crystallographic directions. This crystallographic information suggests that  $\text{PdO}$  is expelled from the  $\text{La}_4\text{PdO}_7$  matrix in certain crystallographic directions when  $\text{La}_4\text{PdO}_7$  is decomposed. Such a mechanism would also promote the formation of nanosized  $\text{Pd}/\text{PdO}$  particles. The ATEM studies indicate that such particles are indeed formed when  $\text{La}_4\text{PdO}_7$  is exposed to car exhaust



Fig. 5. A TEM image of an  $\text{La}_4\text{PdO}_7$  particle exposed to oxidising atmosphere ( $S = 1.1$ ) having  $\text{Pd}$  particles on its surface.

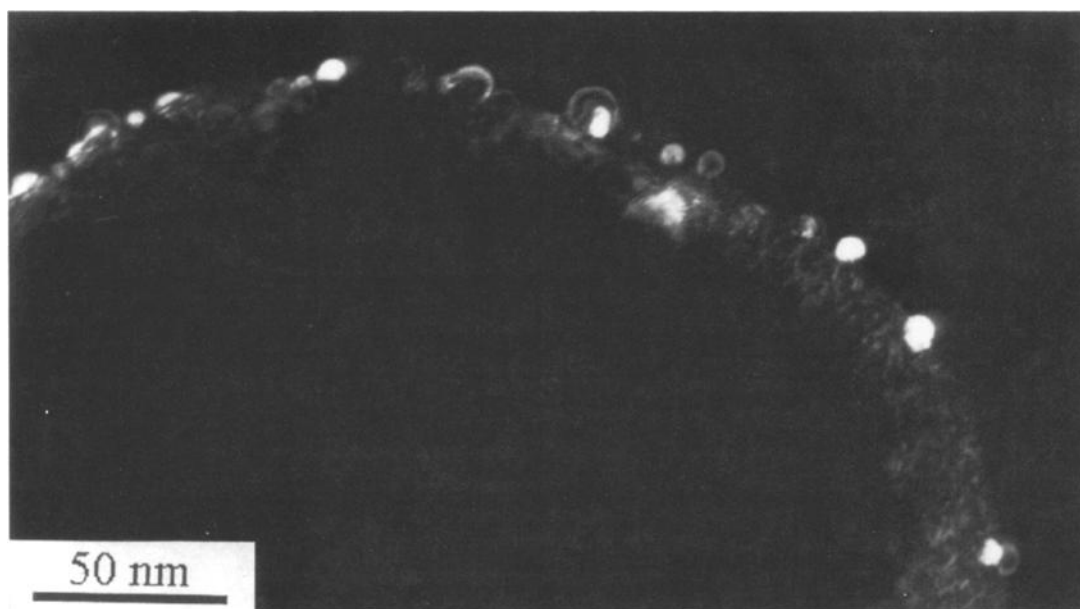


Fig. 6. A TEM image obtained in dark-field mode of an  $\text{La}_4\text{PdO}_7$  particle exposed to reducing atmosphere ( $S = 0.9$ ).

atmosphere. The X-ray powder pattern of activated  $\text{La}_4\text{PdO}_7$  did not contain any reflections which could be ascribed to Pd and/or PdO indicating that these particles

are too small to be detected by this technique or are amorphous.

Our FT-IR studies suggested that the catalytically active component in our catalyst is Pd rather than PdO, in agreement with the findings by Sugai et al. [13] and Graham [14]. The light-off curves given in figs. 1 and 2 can thus all be interpreted in terms of  $\text{La}_4\text{PdO}_7$  decomposing into  $\text{La}_2\text{O}_3$  and PdO, the latter being reduced to Pd. The oxidation of CO and  $\text{C}_3\text{H}_6$  and reduction of NO are thus catalytically activated by these nano-sized Pd particles. The decomposition of  $\text{La}_4\text{PdO}_7$  occurs both in reducing ( $S = 0.9$ ) and oxidizing ( $S = 1.1$ ) atmospheres. These studies show that the thermal stability of  $\text{La}_4\text{PdO}_7$  is dependent on the partial pressure of oxygen in the surrounding atmosphere as well as on the temperature. To the extent that one can prepare sub-micron particles of  $\text{La}_4\text{PdO}_7$  and design the thermal stability of  $\text{La}_4\text{PdO}_7$ , i.e. by replacing some of the La ions by Sm and/or Nd ions, one should be able to prepare a catalyst containing many nano-sized Pd particles. Exploratory experiments along these lines as well as studies of the thermal stability of  $\text{La}_2\text{Pd}_2\text{O}_5$  and  $\text{La}_2\text{PdO}_4$  and similar compounds are being undertaken.

Finally, this decomposition process ought to imply that the Pd particles are well anchored to the substrate, i.e. the tendency of the catalytically active component to form larger aggregates, which in turn decreases the efficiency of the converter, ought to be less pronounced here than in converters where Pd is deposited onto the wash-coat by a dip-coating technique. Anyhow, if the activity of a catalyst based on this material is decreased for one reason or another, it can easily be regenerated by subsequent heat treatment in air at elevated temperatures, which yields  $\text{La}_4\text{PdO}_7$  that can be re-activated.

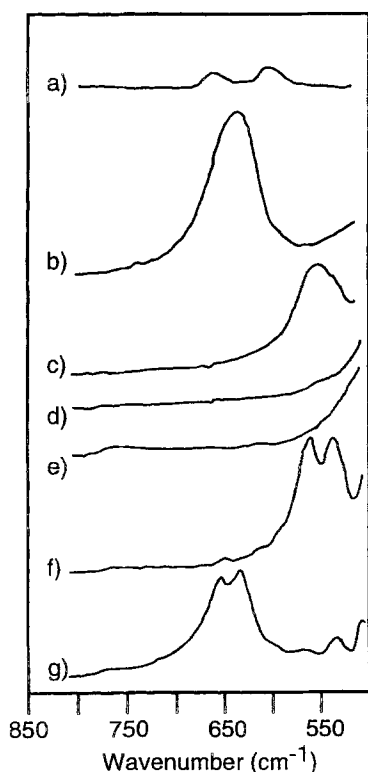


Fig. 7. FT-IR spectra of (a) PdO, (b)  $\text{La}(\text{OH})_3$ , (c)  $\text{La}_4\text{PdO}_7$  as prepared, (d)  $\text{La}_2\text{O}_3$ , (e)  $\text{La}_4\text{PdO}_7$  activated in reducing atmosphere, (f)  $\text{La}_4\text{PdO}_7$  activated in oxidizing atmosphere ( $S = 1.1$ ) and (g)  $\text{La}_4\text{PdO}_7$  activated in reducing atmosphere ( $S = 0.9$ ) and stored in hexane.

## Acknowledgement

This work has been financially supported by the Swedish National Research Council and by the Swedish Board for Industrial and Technical Development.

## References

- [1] H. Muraki, K. Yokota and Y. Fujitani, *Appl. Catal.* 48 (1989) 93.
- [2] T.E. Hoost and K. Otto, *Appl. Catal. A* 92 (1992) 39.
- [3] H. Shinjoh, S. Matsuura and H. Hirayama, *Proc. 73rd CTASJ Meeting*, Abstract No. 1B14, Vol. 36, No. 2 (1994) p. 133.
- [4] L. Fan and K. Fujimoto, *Chem. Lett.* (1994) 105.
- [5] M. Skoglundh, H. Johansson, L. Löwendahl, K. Jansson, L. Dahl and B. Hirschauer, *Appl. Catal. B*, in press.
- [6] H. Muraki, H. Shinjoh and Y. Fujitani, *Appl. Catal.* 22 (1986) 325.
- [7] B.G. Kakhan, V.B. Lazarev and I.S. Shaplygin, *Russian J. Inorg. Chem.* 27 (1982) 1180.
- [8] I.-M. Axelsson, L. Löwendahl and J.-E. Otterstedt, *Appl. Catal.* 44 (1988) 251.
- [9] K.-E. Johansson, T. Palm and P.-E. Werner, *J. Phys.* E3 (1980) 1289.
- [10] H. Muraki, H. Shinjoh, H. Sobukawa, K. Yokota and Y. Fujitani, *Ind. Eng. Chem. Proc. Res. Dev.* 25 (1986) 202.
- [11] J.P. Attfield and G. Férey, *J. Solid State Chem.* 80 (1989) 286.
- [12] J.P. Attfield, *Acta Cryst. B* 44 (1988) 563.
- [13] S. Sugai, H. Watanabe, T. Kioka, H. Miki and K. Kawasaki, *Surf. Sci.* 259 (1991).
- [14] G.W. Graham, *Surf. Sci.* 268 (1992) 25.